RESEARCH ADVANCE

Cell cycle-coupled CK1δ turnover, autoinhibition, and activity

Fidel Emmanuel Serrano, Bianca Ruppert, Axel CR Diernfellner, Michael Brunner*

Heidelberg University Biochemistry Center, Heidelberg, Germany

eLife Assessment

This manuscript presents **valuable** experimental results describing the localisation and regulation of casein kinase CK1δ during the cell cycle. During the G2 phase of the cell cycle, the autophosphorylation of the C-terminal tail stabilises and inhibits the kinase which might protect CK1δ in the subsequent G1 phase. The results may be of interest to researchers working on casein kinase function and regulation but due to lack of some controls remain **incomplete**.
[Editors' note: this paper was reviewed by Review Commons.]

Abstract Casein kinase 1δ (CK1δ) is a ubiquitously expressed kinase involved in diverse cellular processes, including cell-cycle regulation. CK1δ activity is attenuated by (auto)phosphorylation. However, inhibitory phosphorylation is efficiently opposed by cellular phosphatases as CK1δ accumulates in its hypophosphorylated, active state. CK1δ is a target of the nuclear ubiquitin ligase APC/C-CDH1, yet the kinase is apparently stable. Thus, the physiological relevance of CK1δ (auto) phosphorylation, autoinhibition, and regulated turnover has remained unclear. Previously, we showed that CK1δ is dynamically regulated in a manner that is dependent on kinase activity, subcellular localization, and interaction with its binding partners, such as PER2 (Serrano et al., 2026). Here, we show that CK1δ activity and abundance are additionally coordinated in a cell cycle-dependent manner. During G1, assembled CK1δ kinase is stable while free active kinase is degraded. In S phase, unassembled CK1δ seems to be no longer degraded, likely to support functions in DNA damage signaling. Upon mitotic entry, the downregulation of phosphatases promotes CK1δ (auto) phosphorylation and consequent autoinhibition, thereby preserving a pool of kinase to rapidly re-establish the post-mitotic steady state.

***For correspondence:** michael.brunner@bzh.uni-heidelberg.de

Competing interest: The authors declare that no competing interests exist.

Funding: See page 18

Preprint posted
16 June 2026
Sent for Review
12 July 2026
Reviewed preprint v1
21 August 2026
Reviewed preprint v2
08 October 2026
Version of Record
28 October 2026

Reviewing Editor: Volker Dötsch, Goethe University Frankfurt, Germany

© Copyright Serrano *et al*. This article is distributed under the terms of the Creative Commons Attribution License, which permits unrestricted use and redistribution provided that the original author and source are credited.

Introduction

Casein kinase 1 (CK1) is an evolutionarily conserved serine/threonine kinase found throughout the eukaryotic lineage (***Gross and Anderson, 1998***), with homologs in yeast (***DeMaggio et al., 1992***), fungi (***Görl et al., 2001***), plants (***Klimczak et al., 1995***), and animals (***Etchegaray et al., 2009***). CK1 isoforms act as effectors in a variety of cellular signaling pathways (***Schittek and Sinnberg, 2014***; ***Xu et al., 2019***). All members of the CK1 family share a highly conserved, structured catalytic domain and a divergent, largely disordered C-terminal tail (***Graves and Roach, 1995***; ***Cegielska et al., 1998***). CK1 enzymes are phosphate-directed kinases displaying high affinity for motifs pre-phosphorylated (primed) at the –3 and, to a lesser extent, also the –4 position with the consensus pS/T-X-X-(X)-S/T but display much lower activity toward unprimed sites (***Narasimamurthy et al., 2018***; ***Flotow et al., 1990***; ***Marzoll et al., 2022***). This specificity is conferred by a dedicated phosphate-binding pocket that correctly orients the primed substrate (***Flotow et al., 1990***). CK1s are considered constitutively active because they do not have regulatory subunits and are not activated by phosphorylation of their activation loop (***Johnson et al., 1996***).

Among the seven CK1 isoforms in humans (α, β, γ1, γ2, γ3, δ, and ε), CK1δ and CK1ε play crucial roles in regulating the circadian clock (***Etchegaray et al., 2009***; ***Narasimamurthy et al., 2018***; ***Marzoll et al., 2022***), cytoskeletal organization (***Behrend et al., 2000***; ***Greer et al., 2014***), cell cycle (***Johnson et al., 2013***; ***Penas et al., 2014***), and development (***Gao et al., 2002***; ***Jiang et al., 2014***; ***Zhao et al., 2010***). CK1δ and CK1ε activity is attenuated by phosphorylation of their C-terminal tail (***Graves and Roach, 1995***; ***Cegielska et al., 1998***). Autoinhibition occurs via a competitive mechanism in which the phosphorylated tail blocks the active site (***Harold et al., 2024***; ***Cullati et al., 2024***). Inhibitory tail phosphorylation is mediated by autophosphorylation and phosphorylation by other cellular kinases (***Xu et al., 2019***; ***Marzoll et al., 2022***). Although C-terminal tail phosphorylation inhibits CK1δ/ε in vitro, the kinases undergo futile cycles of phosphorylation and dephosphorylation (***Rivers et al., 1998***), keeping the kinase in a dephosphorylated, active state (***Liu et al., 2002***). CK1δ/ε activity is controlled by several mechanisms, including sequestration (***Xu et al., 2019***), leaving the physiological significance of this inhibitory mechanism unclear.

CK1δ is shuttling between nucleus and cytoplasm and localizes dynamically to the centrosome and pericentrosomal region (***Greer et al., 2014***; ***Sillibourne et al., 2002***; ***Greer and Rubin, 2011***). Catalytically inactive CK1δ mutants accumulate in the nucleus, and nuclear export of CK1δ depends on kinase activity (***Milne et al., 2001***; ***Serrano et al., 2026***). CK1δ is a target of the nuclear ubiquitin ligase anaphase-promoting complex/cyclosome in association with its coactivator CDH1 (APC/C-CDH1) (***Penas et al., 2015***), which is active from late anaphase/telophase through G1 and inactivated when the cell cycle progresses into S phase (***Sivakumar and Gorbsky, 2015***). Yet, CK1δ appears to be stable (***Lee et al., 2001***; ***Cao et al., 2021***), raising the question about the physiological conditions under which APC/C-CDH1 targets the kinase.

We have recently analyzed the posttranslational regulation of CK1δ in unsynchronized cells, which are mainly in the G1 phase of the cell cycle (***Serrano et al., 2026***). These findings indicate that CK1δ is stabilized through assembly with binding partners such as the circadian clock protein PER2. In contrast, unassembled CK1δ, which accumulates at detectable levels upon overexpression, is rapidly degraded. This suggests that APC/C-CDH1 selectively targets the unassembled kinase, thereby limiting aberrant CK1δ activity. Here, we expand our analysis of CK1δ regulation in G1 and investigate how CK1δ stability and localization are controlled across the cell cycle.

Results

Subcellular distribution of CK1δ is dynamic

We have recently shown that CK1δ expressed at physiological levels is stable, while overexpressed CK1δ, which is not assembled with binding partners such as PERIOD2, is rapidly degraded, preferentially in the nucleus in a manner dependent on its kinase activity (***Serrano et al., 2026***). To characterize in more detail the subcellular dynamics, synthesis, and turnover of endogenous CK1δ we performed immunofluorescence (IF) of U2OStx cells. In untreated cells, CK1δ was highly concentrated in the pericentrosomal region (***Figure 1A and C***), consistent with its reported localization at the centrosome and Golgi apparatus (***Xu et al., 2019***; ***Roth et al., 2022***), and was also detectable in the nucleus, consistent with its reported association with PERIOD proteins (***Cao et al., 2021***).

We then asked whether the subcellular localization of CK1δ is static or dynamic. It has been shown that catalytically inactive CK1δ mutants accumulate in the nucleus (***Milne et al., 2001***), and we have previously shown that kinase inhibition with PF670462, a specific CK1δ/ε inhibitor (***Badura et al., 2007***), inhibits nuclear export of CK1δ and, in addition, protects the kinase from degradation. Therefore, to trap and stabilize shuttling CK1δ in the nucleus, U2OStx cells were treated for 4 hr with PF670462 together with cycloheximide (CHX) to distinguish relocalization from de novo protein synthesis. Under these conditions, the localization of CK1δ at the pericentrosomal region was reduced, and the kinase accumulated in the nucleus (***Figure 1A and C***). These data demonstrate that the pericentrosomal localization of CK1δ is dynamic and in equilibrium with the nuclear pool. A fraction of CK1δ remained associated with the pericentrosomal region after the 4 hr treatment with PF670462 (***Figure 1C***).

Next, we analyzed U2OStx cells stably overexpressing doxycycline (DOX)-inducible FLAG-tagged CK1δ. Expression of CK1δ-FLAG was induced for 24 hr with DOX to generate a pool of unassembled kinase and analyzed by IF. Despite overexpression, the subcellular distribution of CK1δ-FLAG was similar to that of CK1δ in control cells, displaying pronounced concentration of CK1δ-FLAG in the

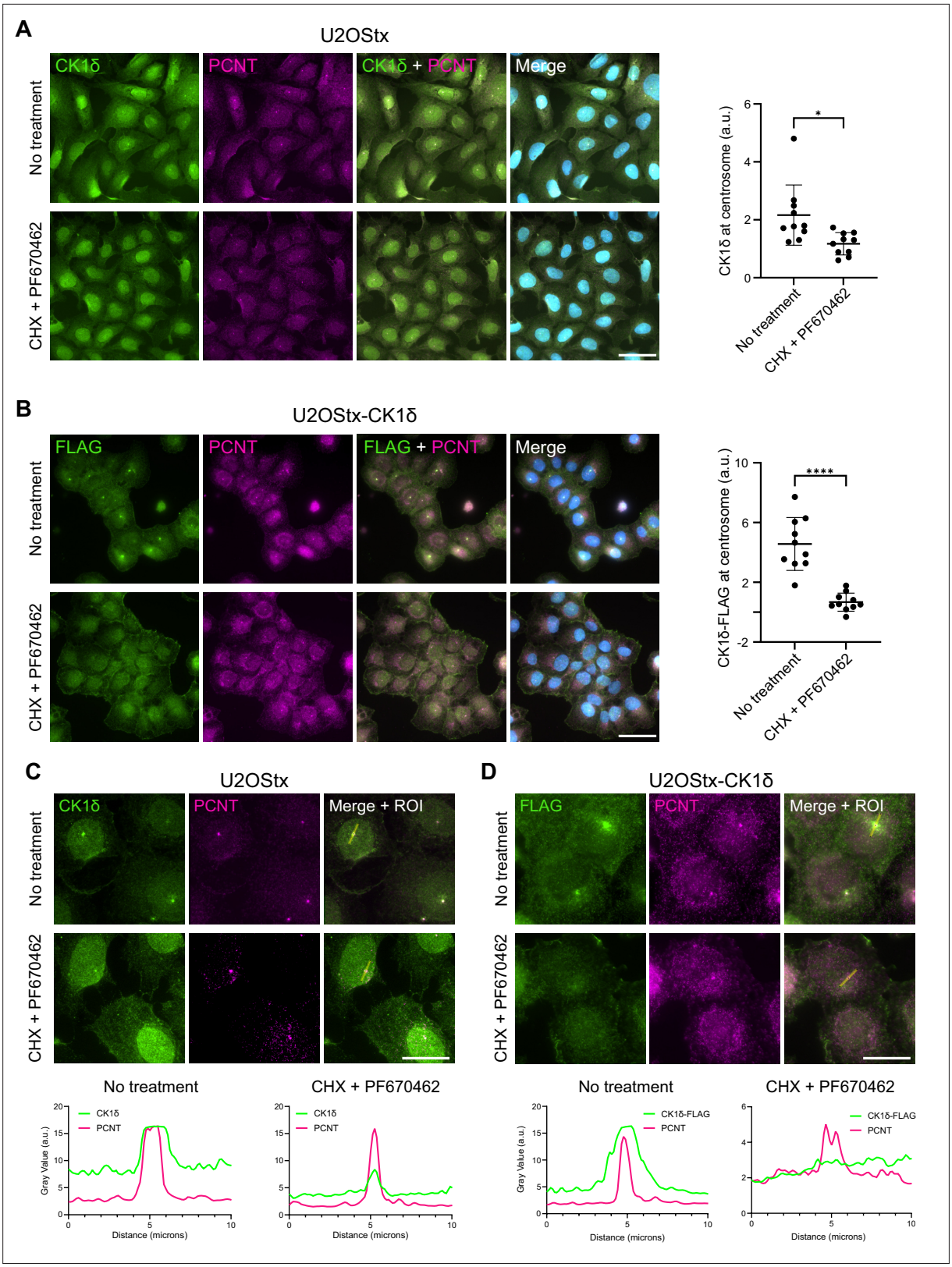


Figure 1. CK1δ inhibition results in decreased centrosomal localization. (**A**) U2OStx cells were treated with a combination of cycloheximide (CHX) and PF670462 for 4 hr to inhibit protein synthesis and kinase activity or left untreated. Endogenous CK1δ and pericentrin (PCNT) were detected by immunofluorescence (IF). Green (AF488): anti-CK1δ, magenta (Cy3): anti-PCNT. Nuclei were identified with DAPI. In untreated cells, CK1δ exhibited clear nuclear and pericentrosomal staining. In CHX+PF670462-treated cells, pericentrosomal localization of CK1δ was decreased and CK1δ accumulated

Figure 1 continued on next page

Figure 1 continued

in the nucleus. Scale bar = 50 μm. Right panel: Density above surrounding background of CK1δ at pericentrosomal region. Quantification of n=10 cells, Welch's t-test. * indicates p-value<0.05. (**B**) Doxycycline (DOX)-induced U2OStx_CK1δ cells were either left untreated or treated with CHX and PF670462 for 4 hr and analyzed as described above. Green (AF488): CK1δ-FLAG was detected with anti-FLAG antibody. Magenta (CY3): anti-PCNT. In untreated cells, CK1δ-FLAG was concentrated at the pericentrosomal region. In CHX+PF670462-treated cells, pericentrosomal localization of CK1δ-FLAG was decreased and CK1δ-FLAG accumulated in the nucleus. Right panel: Density above surrounding background of CK1δ-FLAG at pericentrosomal region. Quantification of n=10 cells. Welch's t-test. **** indicates p-value<0.0001. U2OStx cells (**C**) and DOX-induced U2OStx_CK1δ cells (**D**) were analyzed as described in (**A**) and (**B**), respectively. Fiji-based multi-channel line plot analysis showing the fluorescence intensity profiles of CK1δ (**C**) and CK1δ-FLAG (**D**) relative to PCNT along the indicated region of interest (ROI) in representative untreated cells and cells treated with CHX or PF670462. Scale bar = 20 μm.

The online version of this article includes the following source data for figure 1:

Source data 1. Data underlying the plot in ***Figure 1A***.

Source data 2. Data underlying the plot in ***Figure 1B***.

Source data 3. Data underlying the plot in ***Figure 1C***.

Source data 4. Data underlying the plot in ***Figure 1D***.

pericentrosomal region (***Figure 1B***). Treatment with PF670462 resulted in nuclear accumulation of CK1δ-FLAG and reduction of pericentrosomal staining (***Figure 1B and D***). These data indicate that pericentrosomal and nuclear CK1δ exist in a dynamic equilibrium, regardless of whether the kinase is expressed at physiological levels or overexpressed.

Thus, at steady state, the subcellular levels of endogenous or overexpressed CK1δ are not static but are dynamically maintained by the balance between subcellular shuttling, binding equilibria with the pericentrosomal region. We have recently shown that unassembled CK1δ is rapidly degraded in the nucleus (***Serrano et al., 2026***). Our data suggest that under physiological expression levels, rebinding of CK1δ to the pericentrosomal region constitutes the dominant pathway, effectively outcompeting nuclear degradation, while overexpression promotes degradation of free nuclear CK1δ. Such a mechanism would enable continuous monitoring and regulation of CK1δ levels while maintaining a low abundance of unassembled, potentially harmful kinase. Because free CK1δ levels are kept low and pericentrosomal binding sites are not saturated (***Serrano et al., 2026***), the pericentrosomal CK1δ pool may function as a buffered reservoir that can supply newly emerging binding partners such as PERIOD proteins when they accumulate at higher levels than free CK1δ.

To test this hypothesis, we employed U2OStx cells stably expressing mKate2-tagged cryptochrome 1 (mK2-CRY1). These U2OStx-mK2-CRY1 cells were transfected with PER2 to rapidly overexpress a binding partner of CK1δ. As recently shown (***Serrano et al., 2026***), overexpressed PER2 and mK2-CRY1 mutually stabilize each other and co-accumulate in nuclear foci, whereas in untransfected cells mK2-CRY1 alone is unstable, expressed at a low level, and homogeneously distributed throughout the nucleus (***Figure 2A***). Thus, the formation of nuclear mK2-CRY1 foci serves as an indicator of PER2 transfection (***Serrano et al., 2026***). Because U2OStx cells exhibit low transfection efficiency, only a fraction of U2OS-mK2-CRY1 cells expressed PER2. This allowed a side-by-side comparison between endogenous CK1δ in PER2-expressing cells identified by nuclear mK2-CRY1 foci from non-expressing cells within the same population. In untransfected cells, endogenous CK1δ was concentrated at the single centrosome (***Figure 2B***, red arrows). In contrast, in PER2-transfected cells, CK1δ accumulated at elevated levels and colocalized with mK2-CRY1 in PER2-dependent nuclear foci (***Figure 2B***). Notably, all nuclear CK1δ foci were mK2-CRY1 positive, whereas CK1δ foci lacking mK2-CRY1, which would indicate pericentrosomal localization of CK1δ, were not detected in PER2-transfected cells. This change in CK1δ localization upon formation of nuclear mK2-CRY1 foci is consistent and can be seen in multiple fields of view. Together, these findings suggest that PER2 overexpression competes for CK1δ binding and, when expressed at very high levels, can even displace CK1δ from the pericentrosomal region.

Dephosphorylation of CK1δ by cellular phosphatases

Phosphorylation of CK1δ at the kinase C-terminal tail can be stabilized and detected by treating cells with phosphatase inhibitors (***Ishihara et al., 1989***). We compared the kinetics of tail phosphorylation upon treatment of cells with calyculin A (CalA), a potent inhibitor of the protein phosphatases PP1 and PP2A, and okadaic acid (OA), which inhibits PP2A more effectively than PP1 (***Swingle et al.,***

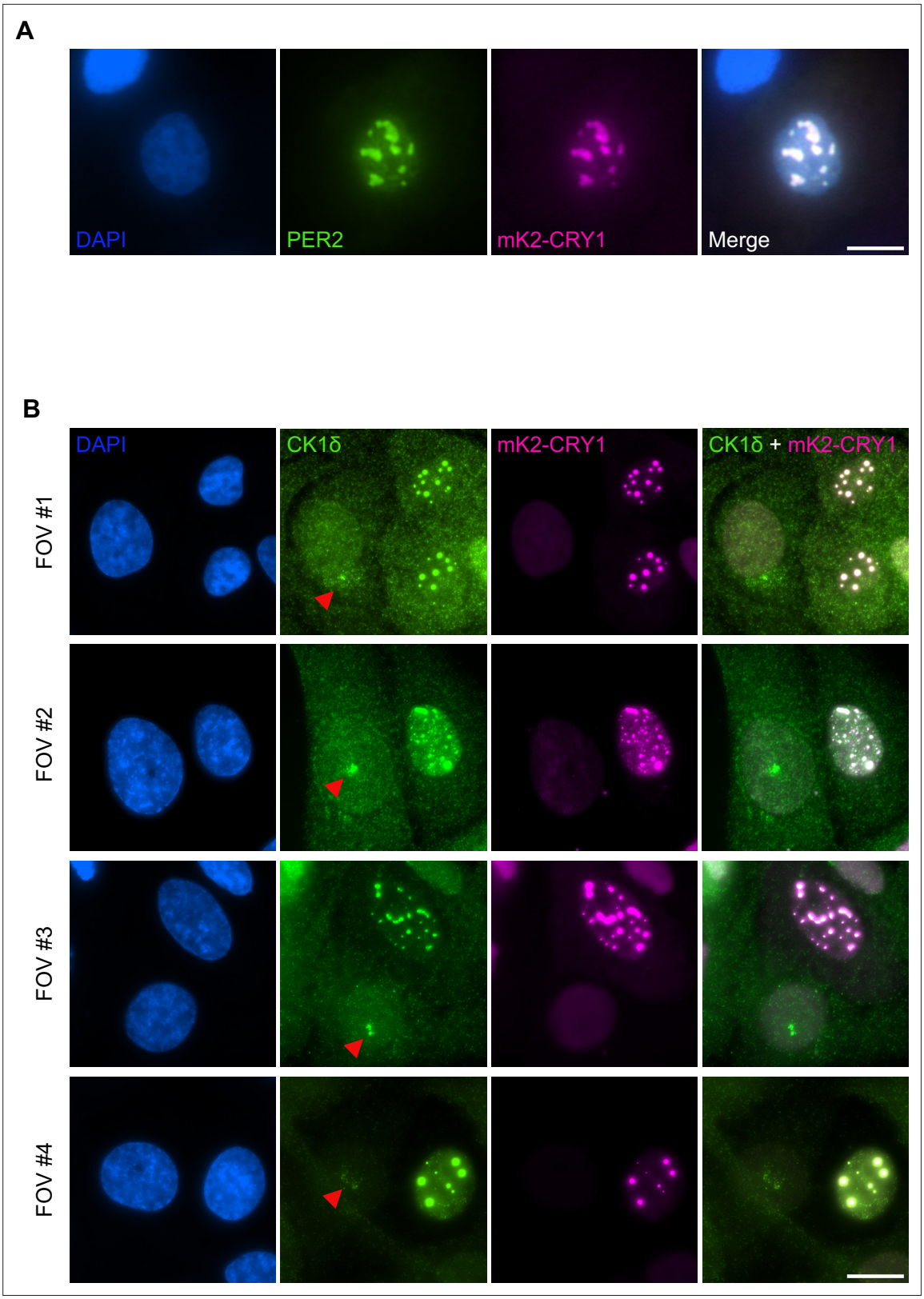


Figure 2. PER2 overexpression displaces CK1δ from the centrosome. U2OStx_mK2-CRY1 cells were transfected with PER2, followed by doxycycline (DOX) induction. (**A**) Immunofluorescence (IF) for PER2 shows the formation of nuclear foci containing both overexpressed PER2 and mK2-CRY1 as reported previously (***Serrano et al., 2026***). Scale bar = 20 μm. (**B**) IF for CK1δ shows that the kinase expressed from its endogenous locus is recruited to the nuclear PER2-CRY1 foci and depleted from the pericentrosomal region, in agreement with previous observations (***Serrano et al., 2026***). Four

Figure 2 continued on next page

Figure 2 continued

fields of view (FOVs) are shown. Presence and absence of nuclear mK2-CRY1 foci indicate PER2-transfected and untransfected cells, respectively. Pericentrosomal CK1δ localization, accessed by CK1δ-positive (green) and CRY1-negative (magenta) foci, was observed in all untransfected cells examined (50 out of 50 cells evaluated). In PER2 and CRY1-expressing cells, CK1δ accumulated in CRY1-positive (magenta) nuclear foci. No cell (0 out of 15 cells evaluated) displayed pericentrosomal localization of CK1δ (CRY1-negative focus). Fisher's exact test, $p=4.8 \times 10^{-15}$. Scale bar = 20 μm.

2006). For this purpose, we used U2OStx stably expressing under a DOX-inducible promoter either FLAG-tagged wild-type CK1δ or its catalytically inactive (kinase-dead) version, CK1δ-K38R (***Marzoll et al., 2022***). In U2OStx_CK1δ cells, both CalA and OA inhibited CK1δ dephosphorylation and led to the accumulation of elevated levels of hyperphosphorylated CK1δ (***Figure 3A***), suggesting that phosphorylation protects the overexpressed kinase from degradation. CalA does not inhibit PP2C or protein tyrosine phosphatases and is largely ineffective against PP2B and PP7. Thus, the sensitivity of CK1δ dephosphorylation to CalA suggests PP1, PP2A, PP4, and PP5 as likely candidates contributing to dephosphorylation (***Swingle et al., 2006***). Although sensitivity to CalA and OA cannot rigorously distinguish among these phosphatases, the high OA concentrations required to inhibit CK1δ dephosphorylation suggest the involvement of PP1, which is 10- to 100-fold less sensitive to OA than PP2A, PP4, or PP5 (***Ishihara et al., 1989***; ***Swingle et al., 2006***). Thus, CK1δ is actively maintained in a dephosphorylated state, most likely through the contribution of PP1, with possible additional contributions from PP2A, PP4, and PP5. PP1 has previously been suggested as a major phosphatase of CK1δ/ε (***Lee et al., 2011***). Notably, PP1, PP2A, and PP4 activities are downregulated during mitosis (***Nasa and Kettenbach, 2018***; ***Kim et al., 2016***), pointing to a potential physiological role for CK1δ tail phosphorylation and autoinhibition during this stage of the cell cycle.

To analyze whether the electrophoretic mobility shift induced by CalA treatment was indeed caused by phosphorylation of the CK1δ tail, we generated a U2OStx cell line expressing a CK1δ variant in which all serine and threonine residues in the C-terminal tail were replaced by alanine ($CK1\delta_A$). Treatment of these cells with CalA did not induce an electrophoretic mobility shift of the tail mutant kinase (***Figure 3B***).

To separate autophosphorylation from phosphorylation by other kinases, we examined U2OStx_CK1δ-K38R cells. Upon CalA or OA treatment, the kinase-dead CK1δ-K38R accumulated at elevated levels and was also phosphorylated but to a lesser extent than wild-type CK1δ (***Figure 3C***), suggesting that fewer phosphorylation sites are targeted by other kinases. Because CK1δ-K38R is already rather stable (***Serrano et al., 2026***), the data suggest that partial tail phosphorylation is sufficient to further stabilize CK1δ-K38R. Time course experiments revealed that CK1δ became hyperphosphorylated within 1 hr of CalA treatment, with intermediate phosphorylation states visible at 6 and 20 min (***Figure 3D***), in agreement with previous observations (***Graves and Roach, 1995***). CalA-induced phosphorylation of CK1δ-K38R followed similar kinetics (***Figure 3D***). We noted that treatment with a PPase inhibitor led to increased levels of overexpressed, and thus unassembled, CK1δ (***Figure 3A and D***) as well as CK1δ-K38R (***Figure 3C and D***), suggesting that full or partial phosphorylation of the CK1δ tail stabilizes both active and inactive forms of the kinase.

Tail phosphorylation protects CK1δ/ε from degradation

To examine in more detail how tail phosphorylation affects the turnover of unassembled CK1δ, U2OStx cells stably expressing CK1δ-FLAG were either left untreated or pre-treated for 1 hr with the phosphatase inhibitor CalA, alone or together with PF670462, followed by a 90 min CHX chase. In CHX-treated cells, overexpressed CK1δ was rapidly degraded, with a half-life of approximately 15 min (***Figure 4A***), consistent with our previous findings (***Serrano et al., 2026***). The 1 hr pre-treatment with CalA induced hyperphosphorylation of CK1δ, whereas co-treatment with PF670462 and CalA produced an intermediate phosphorylation state (***Figure 4A***), similar to the CalA-induced phosphorylation of CK1δ-K38R, indicating that PF670462-insensitive kinases targeted a fraction of the phosphorylation sites in CK1δ tail. Both 1 hr pre-treatments resulted in elevated CK1δ expression levels, indicating that most of the newly synthesized overexpressed kinase was degraded in untreated cells. This conclusion was confirmed by the CHX chase. Hyperphosphorylated CK1δ remained stable throughout the CHX chase (***Figure 4A and C***), indicating that tail phosphorylation protects the overexpressed kinase from rapid degradation. CK1δ shares a high degree of sequence identity and potential functional redundancy with CK1ε, with both kinases implicated in circadian clock regulation (***Etchegaray et al., 2009***;

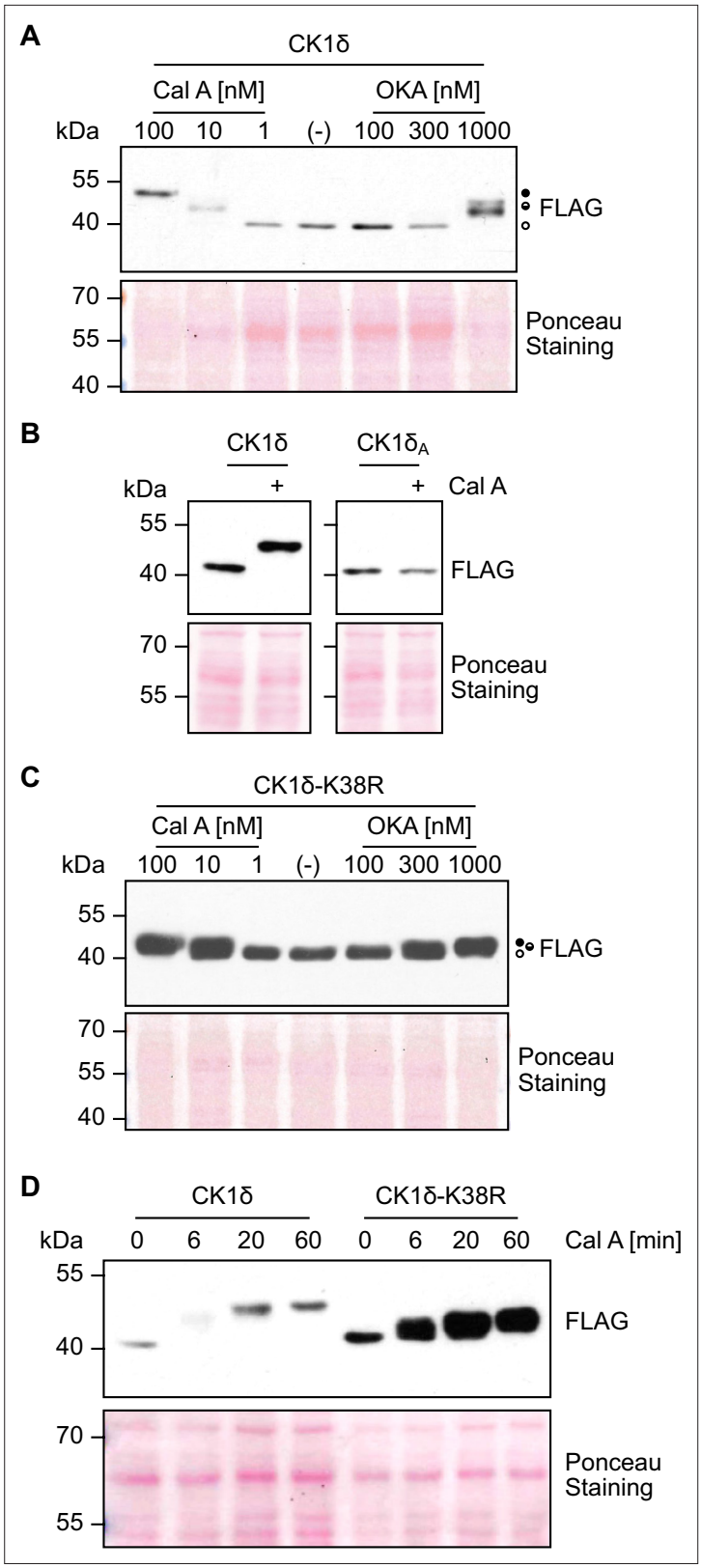


Figure 3. Phosphatase inhibition results in CK1δ phosphorylation. (**A**) Immunoblot analysis of calyculin A (CalA)- and okadaic acid (OA)-induced phosphorylation of CK1δ-FLAG. Phosphorylation of CK1δ is strongly induced by CalA and, albeit with markedly lower efficiency, also by OA. n=3. (**B**) Immunoblot analysis demonstrating the absence of a CalA-induced electrophoretic mobility shift in the CK1δ_A mutant kinase. n=3. (**C**) Immunoblot analysis

Figure 3 continued on next page

Figure 3 continued

of CalA- and OA-induced phosphorylation of kinase-dead CK1δ-K38R. n=3. (**D**) Time course of CalA-induced phosphorylation of CK1δ and CK1δ-K38R. n=3. Ponceau S staining of membranes is shown as loading control.

The online version of this article includes the following source data for figure 3:

Source data 1. Annotated uncropped immunoblots for ***Figure 3***, indicating lane identities and bands used in analysis.

Source data 2. Original uncropped immunoblots for ***Figure 3***.

Takahashi, 2017) and Wnt signaling (***Cruciat, 2014***). Treatment of cells overexpressing FLAG-tagged CK1ε with CHX, CalA, and PF670462 revealed that CK1ε turnover is also regulated in a similar manner to CK1δ (***Figure 4B and D***).

CK1δ is a target of the nuclear ubiquitin ligase APC/C-CDH1 (***Penas et al., 2015***). To directly analyze the subcellular turnover of CK1δ, we employed U2OStx cell lines expressing mNeonGreen-tagged CK1δ fused either to an SV40 NLS or to an HIV-1 NES, which direct the kinase predominantly to the nucleus or cytosol, respectively (***Serrano et al., 2026***). Western blot analysis of CHX-treated cell lines revealed that NLS-mNG-CK1δ was degraded more rapidly than NES-mNG-CK1δ.

Cell-cycle dependence of CK1δ expression and phosphorylation

Because CK1δ has various functions at different stages of the cell cycle, including S phase and mitosis (***Schittek and Sinnberg, 2014***; ***Penas et al., 2014***), we investigated whether the expression and phosphorylation state of CK1δ are regulated in a cell cycle-dependent manner. CK1δ is a target of the nuclear ubiquitin ligase APC/C-CDH1 (***Penas et al., 2015***), which is active from late anaphase/telophase all the way through G1 and inactive in S phase, G2, and mitosis (***Sivakumar and Gorbsky, 2015***). To analyze whether inactivation of APC/C-CDH1 affects expression levels of unassembled CK1δ, U2OStx_CK1δ were arrested at G1/S with a double THY block. The block was then relieved and CK1δ expression was analyzed (***Figure 5A***). CK1δ levels increased after release from the G1/S arrest, compared to non-arrested cells (which are predominantly in G1) and to cells arrested at the G1/S transition (***Figure 5B***). The accumulated CK1δ remained dephosphorylated, indicating that the phosphatases acting on the kinase tail were active during S phase. These findings suggest that overexpressed and thus unassembled CK1δ accumulates in a dephosphorylated, active state and escapes nuclear degradation at cell-cycle states when APC/C-CDH1 is inactive. The data suggest that inactivation of APC/C-CDH1 in S phase may protect free nuclear CK1δ to facilitate its functions in DNA damage repair and checkpoint signaling.

Upon entry into mitosis, the activity of major cellular phosphatases such as PP1 and PP2A is globally attenuated (***Nasa and Kettenbach, 2018***; ***Kim et al., 2016***), while distinct pools of these phosphatases remain active at defined subcellular structures (***Nilsson, 2019***). We reasoned that this inhibition might facilitate the accumulation of phosphorylated CK1δ. To test this, we arrested U2OStx_CK1δ cells at the G1/S boundary using a double THY block, and at G2/M using a THY-nocodazole block followed by mitotic shake-off to enrich for cells in mitosis (***Schorl and Sedivy, 2007***; ***Apraiz et al., 2017***; ***Figure 5C***). CK1δ-FLAG was then analyzed via immunoblotting. In unsynchronized (U) and G1/S-arrested cells, CK1δ was hypo- or unphosphorylated. In contrast, G2/M-arrested cells accumulated tail-phosphorylated CK1δ (***Figure 5D***). Similarly, endogenous CK1δ was hyperphosphorylated upon G2/M arrest of U2OStx control cells while it remained hypophosphorylated in unsynchronized and G1/S-arrested cells (***Figure 5E***).

To assess the localization of CK1δ during mitosis, we performed IF on U2OStx_CK1δ cells staining for the overexpressed kinase. Based on the DAPI staining, we assigned the fixed cells to distinct cell-cycle stages. In G2/prophase, identified by duplicated centrosomes and increased DNA content, CK1δ localized predominantly to structures which correspond to the duplicated centrosomes (***Figure 6A***, first column), consistent with previous reports (***Greer et al., 2014***; ***Sillibourne et al., 2002***). In metaphase and anaphase (***Figure 6A***, second column), characterized by DNA condensation, overexpressed CK1δ localized to centrosomes and polar microtubules, consistent with previous reports on the localization of endogenous kinase (***Behrend et al., 2000***). In addition, a considerable fraction of the overexpressed CK1δ was evenly distributed throughout the cell, suggesting that unassembled CK1δ was not targeted for degradation. During telophase and cytokinesis, as chromosome segregation and

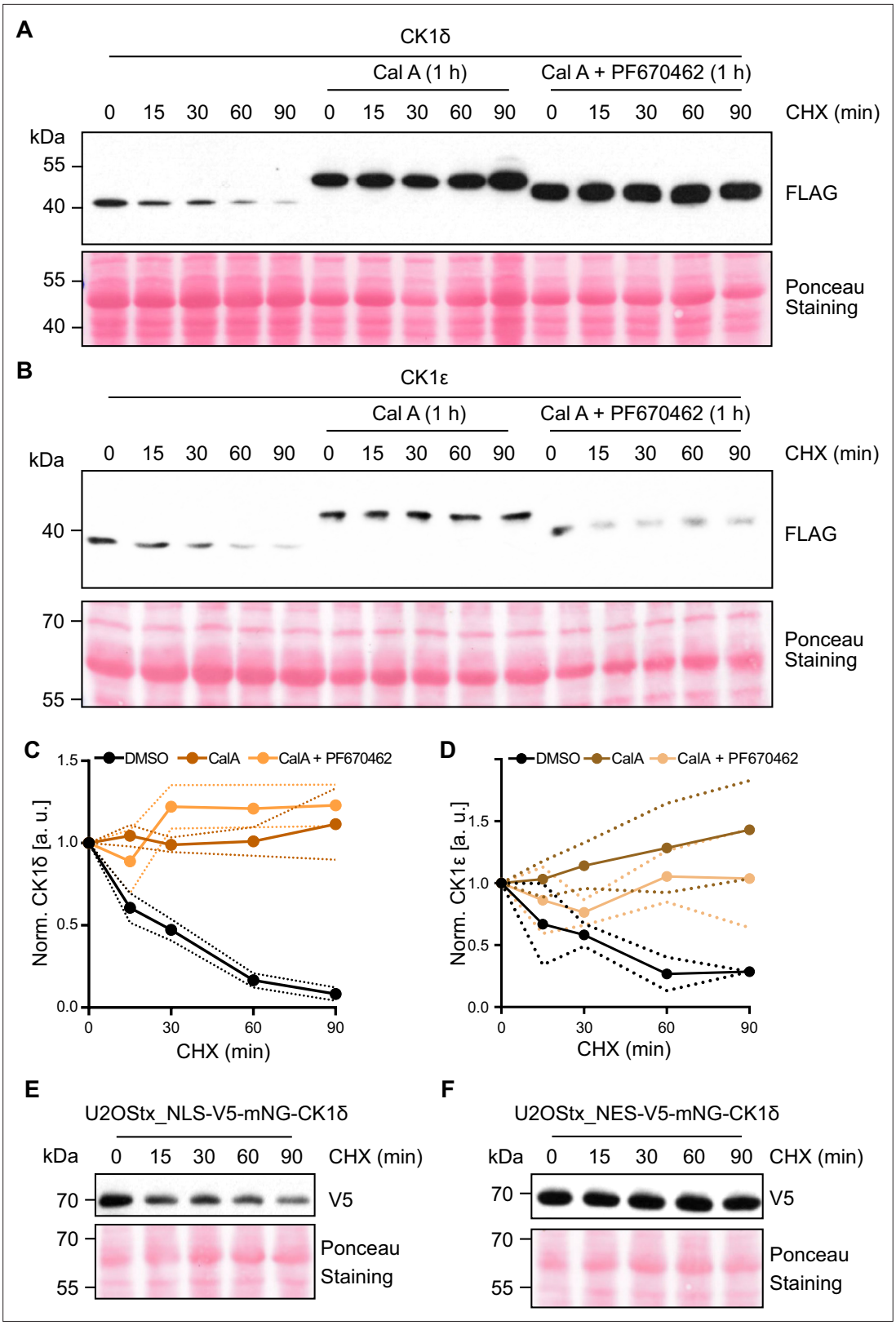


Figure 4. CK1δ/ε phosphorylation stabilizes overexpressed kinase. (**A**) Phosphorylation protects overexpressed CK1δ from degradation. U2OStx_CK1δ cells were incubated with cycloheximide (CHX) (left part) or pre-treated for 1 hr with calyculin A (CalA) (middle part) or with CalA+PF670462 (right part). CK1δ was analyzed at the indicated time points after CHX addition. Overexpressed CK1δ is rapidly degraded. CalA and CalA+PF670462 induce maximal and intermediate phosphorylated CK1δ and stabilize the kinase. n=3. (**B**) CalA and CalA+PF670462 induce phosphorylation of CK1ε and

Figure 4 continued on next page

Figure 4 continued

stabilize the kinase. n=3. (**C**) Densitometric quantification of n=3 western blots (see A) shown as mean ± SD. Overexpressed unphosphorylated CK1δ is degraded with a half-life of about 15 min. Both CalA and CalA+PF670462 treatments stabilize the kinase. (**D**) Densitometric quantification of n=3 western blots (see B) shown as mean ± SD. (**E**) CK1δ is preferentially degraded in the nucleus. U2OStx cells stably expressing NLS-mNG-CK1δ and NES-mNG-CK1δ were incubated with CHX. Samples were analyzed at the indicated time points after CHX addition. Overexpressed NLS-mNG-CK1δ is unstable while NES-mNG-CK1δ is stable. Ponceau S staining of membranes is shown as loading control.

The online version of this article includes the following source data for figure 4:

Source data 1. Annotated uncropped immunoblots for ***Figure 4***, indicating lane identities and bands used in analysis.

Source data 2. Original uncropped immunoblots for ***Figure 4***.

Source data 3. Data underlying the plot in ***Figure 4C***.

Source data 4. Data underlying the plot in ***Figure 4D***.

cell division progressed, CK1δ was diffusely distributed across the dividing cell (***Figure 6A***, third column). Although it is not possible to identify cells that have only recently exited mitosis and entered G1 in fixed samples, all G1 cells displayed a concentration of CK1δ at the pericentrosomal region (***Figure 6A***, fourth column). Similar results were observed when using U2OStx cells and staining for endogenous CK1δ (***Figure 6B***).

Discussion

A central and long-standing question in the regulation of casein kinase 1δ (CK1δ) concerns the physiological role of its autoinhibitory C-terminal tail phosphorylation. Biochemical studies have established that autophosphorylation of the CK1δ tail suppresses catalytic activity, suggesting an intrinsic mechanism for kinase regulation. However, this model appears difficult to reconcile with observations in cells, where CK1δ is found predominantly in a dephosphorylated, and therefore catalytically active state. This discrepancy raises a general conundrum: if CK1δ is constitutively active in vivo, how is its activity effectively regulated, and under what physiological circumstances does tail-mediated autoinhibition become relevant?

A related paradox has emerged in the circadian clock field. CK1δ plays a central role in regulating the stability and nuclear function of circadian PER proteins and is therefore expected to be readily available to ensure robust circadian timekeeping. In principle, CK1δ should not be limiting for PER phosphorylation. Yet, the overexpression of CK1δ consistently accelerates the circadian clock, implying that kinase availability can influence clock speed. This finding suggests that CK1δ activity may be regulated not only by catalytic mechanisms but also by its spatial availability within the cell.

We have recently begun to address this paradox by demonstrating the importance of subcellular localization as it relates to CK1δ function and activity. We have shown that CK1δ is not limiting in the cytosol but becomes limiting in the nucleus in the context of the circadian clock (***Serrano et al., 2026***). This present study provides a potential explanation for how cells reconcile a low synthesis rate of CK1δ and low levels of free kinase with the need for efficient association with binding partners such as PER proteins. Our data indicate that CK1δ is dynamically stored at the pericentrosomal region, potentially forming a buffering pool that can be readily mobilized to bind to its partners. Such a mechanism would allow the cell to maintain low levels of free, potentially harmful, active kinase while simultaneously ensuring that CK1δ is readily available to newly synthesized PER proteins. In this way, pericentrosomal sequestration could function as a buffering system that couples limited CK1δ production to the rhythmically high demand for PER binding and phosphorylation in circadian timekeeping.

Here, we have also addressed the fate of CK1δ across the cell cycle. Because the pool of endogenous free CK1δ is small due to slow synthesis and binding to the pericentrosomal region (***Serrano et al., 2026***), we employed overexpression to analyze localization and degradation of unassembled CK1δ. Our data indicate that unassembled CK1δ is degraded in G1, coinciding with cell-cycle stages in which its nuclear ubiquitin ligase, APC/C-CDH1, is active (***Peters, 2002***; ***Peters, 2006***). We show that hyperphosphorylated CK1δ accumulated in G2/M-arrested cells under both endogenous expression and overexpression conditions. Integrating our findings with previous studies, we propose that in G1 (***Figure 7***), CK1δ is maintained in an active dephosphorylated state. This active CK1δ is dynamically stored at the pericentrosomal region and unassembled molecules are eliminated by the proteasome,

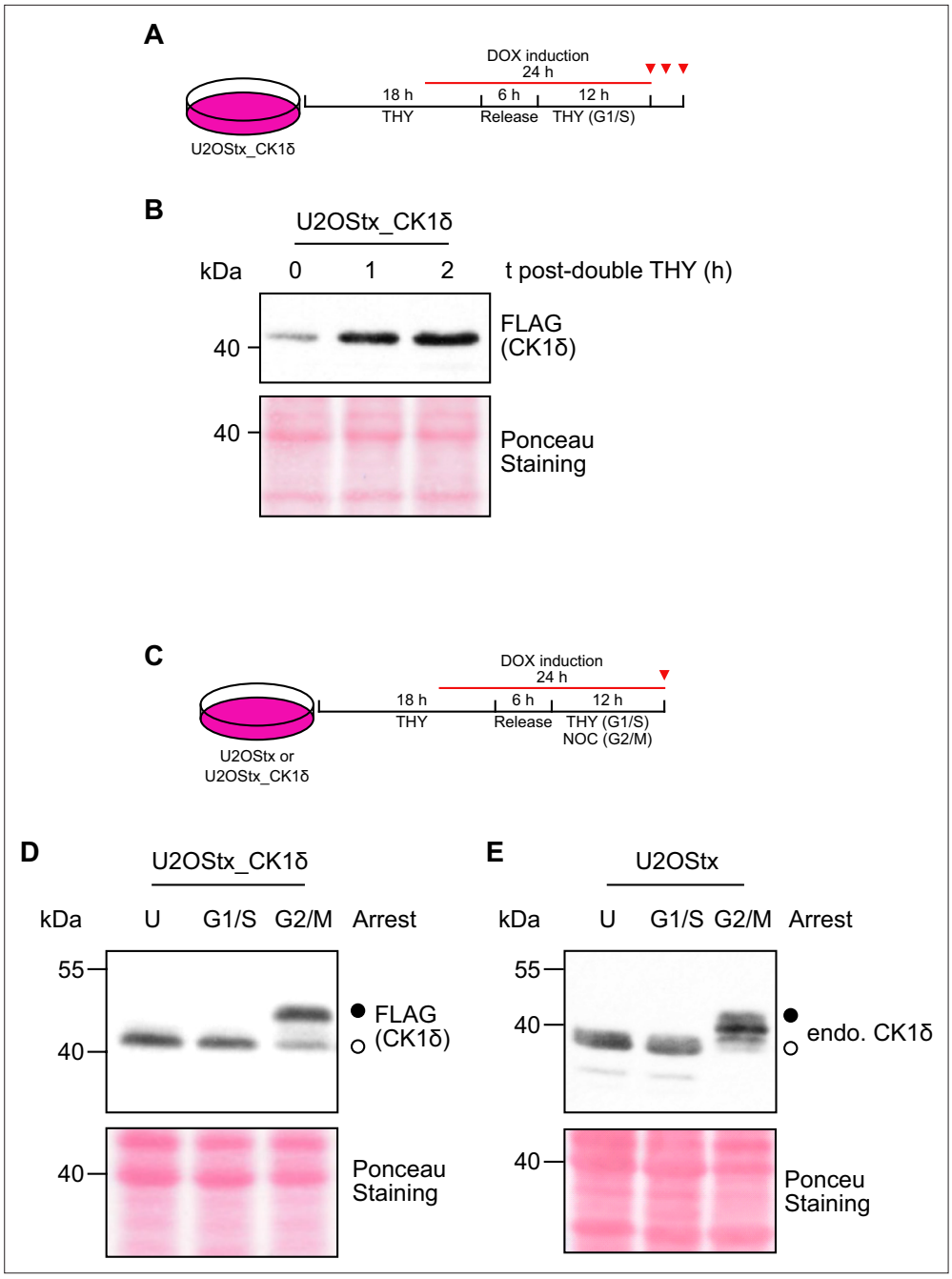


Figure 5. CK1δ is stabilized post-S phase and phosphorylated during G2/M. (**A**) Schematic of S phase arrest and release of U2OStx_CK1δ cells. (**B**) Overexpressed CK1δ accumulates post-S phase release. n=3. (**C**) Schematic of G1/S and G2/M phase arrest of U2OStx_CK1δ or U2OStx cells. (**D, E**) Overexpressed CK1δ in U2OStx_CK1δ cells (**D**) and endogenous CK1δ in U2OStx cells (**E**) are unphosphorylated in unsynchronized and G1/S-arrested cells. G2/M-arrested cells accumulate hyperphosphorylated CK1δ. n=3. Ponceau S staining of membranes is shown as a loading control.

The online version of this article includes the following source data for figure 5:

Source data 1. Annotated uncropped immunoblots for ***Figure 5***, indicating lane identities and bands used in analysis.

Source data 2. Original uncropped immunoblots for ***Figure 5***.

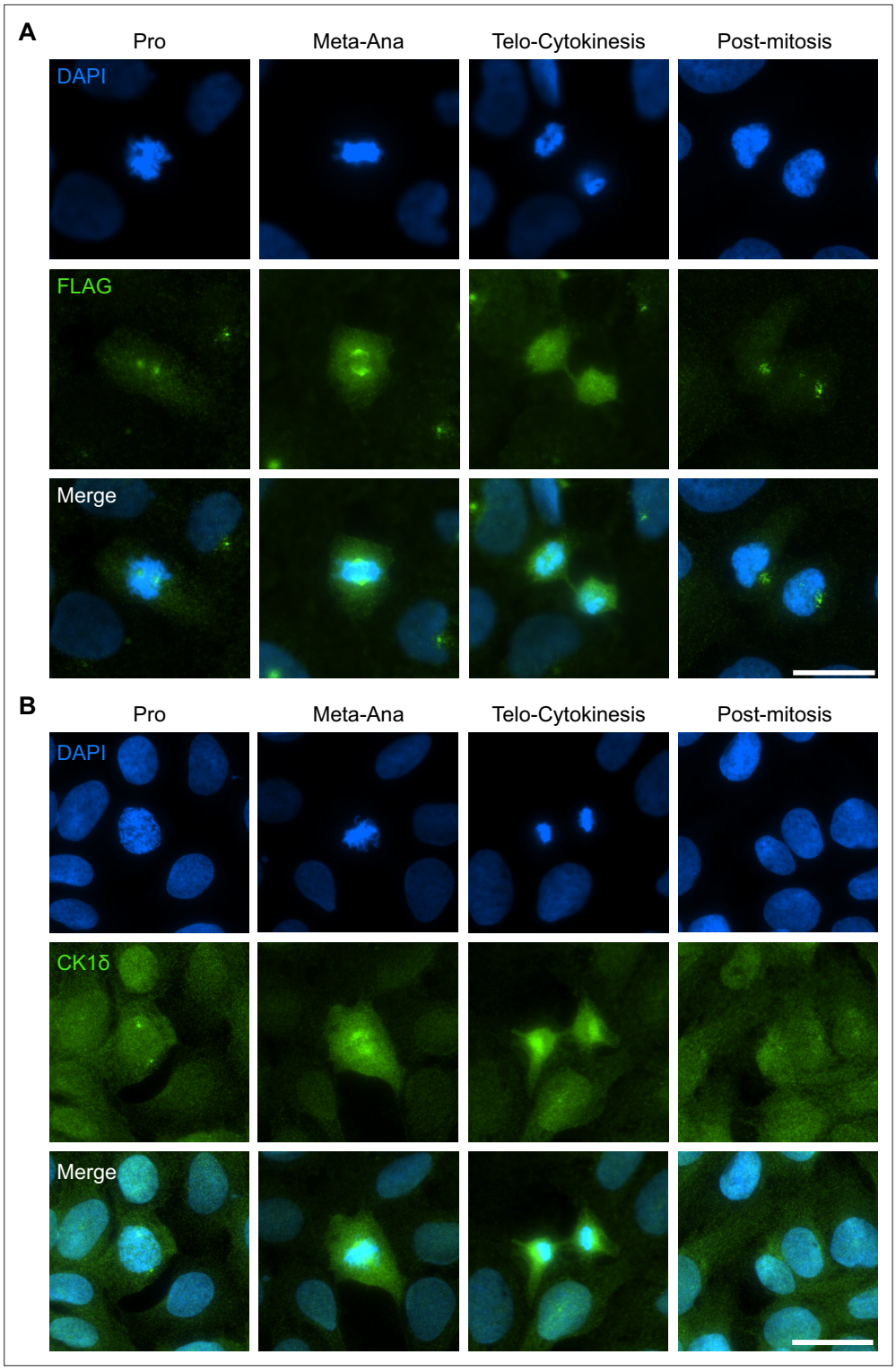


Figure 6. CK1δ localization during mitosis. (**A**) Upper panels: DAPI staining of U2OStx_CK1δ cells was used to identify stages of the cell cycle. Middle panels. Immunofluorescence (IF) analysis of overexpressed CK1δ with FLAG antibody. Lower panels: Merged DAPI and FLAG image. Scale bar = 20 μm. (**B**) Upper panels: DAPI staining of U2OStx cells was used to identify stages of the cell cycle. Middle panels. IF analysis of endogenous CK1δ with anti-CK1δ antibody. Lower panels: Merged DAPI and CK1δ image. Scale bar = 20 μm. Pro: prophase, Meta-Ana: metaphase-anaphase, Telo-Cytokinesis: telophase-cytokinesis.

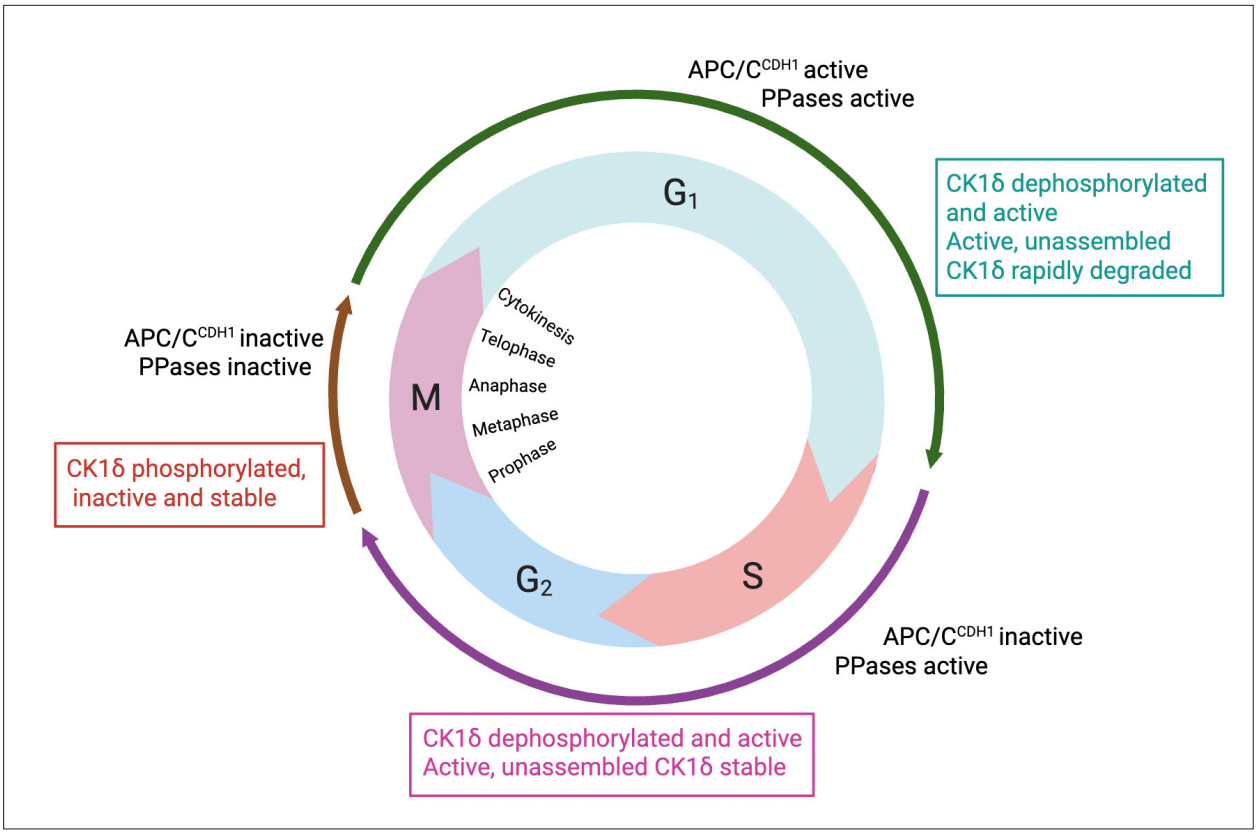


Figure 7. Model of CK1δ regulation over the course of the cell cycle. For details, see main text (discussion section).

primarily in the nucleus through APC/C-CDH1 (***Serrano et al., 2026***; ***Penas et al., 2015***). Because the synthesis rate of CK1δ is low and nuclear kinase is readily exported to the cytosol where it binds to the centrosome and Golgi, the fraction of CK1δ targeted for nuclear degradation is small and not detectable against higher steady-state levels. However, using CK1δ overexpression allows to further uncover this degradation pathway. In S phase, APC/C-CDH1 is inactivated by CDH1 phosphorylation and inhibition of the ubiquitin ligase by its pseudo-substrate (***Sivakumar and Gorbsky, 2015***; ***Machida and Dutta, 2007***). Because phosphatases remain active during S phase, CK1δ is maintained in a dephosphorylated, active state. We propose that unassembled kinase is no longer degraded in the nucleus, likely allowing free kinase to support DNA repair and checkpoint control (***Behrend et al., 2000***; ***Penas et al., 2014***; ***Greer et al., 2017***). CK1 phosphorylation triggers β-TrCP-mediated degradation of MDM2 and activates p53, thereby enhancing p53-dependent responses involved in checkpoint signaling and DNA repair (***Winter et al., 2004***; ***Inuzuka et al., 2010***). Following DNA repair, CK1δ promotes checkpoint exit by phosphorylating WEE1, leading to its β-TrCP-dependent degradation and consequent relief of CDK1 inhibition. CK1δ also supports CHK1 stability during replication stress and, together with CK1ε, phosphorylates Topo IIα to facilitate DNA decatenation in late S/G2, thereby contributing to the orderly resumption of cell-cycle progression (***Penas et al., 2014***; ***Grozav et al., 2009***). Upon mitotic entry, downregulation of phosphatase activity, including PP1 and PP2A (***Nasa and Kettenbach, 2018***; ***Kim et al., 2016***), and activation of mitotic kinases (***Matthews et al., 2022***) facilitate (auto)phosphorylation and autoinhibition of CK1δ, terminating its DNA repair functions. Because CK1δ also contributes to mitotic processes (***Behrend et al., 2000***; ***Penas et al., 2014***; ***Greer and Rubin, 2011***; ***Aquino Perez et al., 2021***; ***Arseni et al., 2024***), a fraction of CK1δ assembled with its binding partners may remain active through locally retained phosphatase activity (***Nilsson, 2019***). The majority of CK1δ, however, becomes phosphorylated and stabilized in an autoinhibited form, safeguarding it for transiently from degradation at mitotic exit, when both phosphatases and APC/C-CDH1 regain activity. At the onset of G1, reactivated CK1δ redistributes preferentially to the pericentrosomal region, while excess dephosphorylated kinase is degraded. By reactivating the safeguarded pool of CK1δ, cells can rapidly re-establish G1-specific steady-state levels without

entirely replenishing the kinase through de novo synthesis, which is rather slow. We have no data regarding the order of events or their kinetics after cells exit mitosis. In particular, we do not know how rapidly CK1δ is dephosphorylated by reactivated phosphatases nor how efficiently it associates with pericentrosomal-binding sites to escape degradation by reactivated APC/C-CDH1. Furthermore, our data do not address whether and how tail phosphorylation regulates CK1δ in G1. However, the bulk of CK1δ remains dephosphorylated in G1, indicating that tail phosphorylation is transient. Together, our findings reveal that the activity and abundance of dephosphorylated and phosphorylated CK1δ are regulated in a cell cycle-dependent manner (***Figure 7***), suggesting distinct physiological functions associated with each phosphorylation state of the kinase. Although our model integrates the new findings reported here together with the data on the regulation of CK1δ in G1 (***Serrano et al., 2026***) and the broader body of knowledge regarding both CK1δ biology and cell-cycle regulation, it is far from complete, and many important questions remain open. However, the model offers plausible novel concepts and mechanistic ideas that provide a basis for further investigation and discussion.

Materials and methods

Key resources table

Reagent type (species) or resource	Designation	Source or reference	Identifiers	Additional information
Cell line (*Homo sapiens*)	U2OStx	Life Technologies	R712-07	
Cell line (*Homo sapiens*)	HEK293T	ATCC	CRL-3216	
Antibody	Anti-CK1δ, mouse monoclonal	abcam	ab85320, AF12G4, RRID:AB_1860174	IF: 1:1000 IB: 1:5000
Antibody	Anti-PCNT, rabbit polyclonal	abcam	ab4448, RRID:AB_304461, generous gift from Dr. Cornelia Sala and Prof. Elmar Schiebel	IF: 1:500
Antibody	Anti-FLAG, mouse monoclonal	Sigma-Aldrich	F3165, RRID:AB_259529	IB: 1:5000 IF: 1:200
Antibody	Anti-PER2, rabbit polyclonal	Pineda Antikörper-Service	Rabbit sera purified in-house	1:50
Antibody	Anti-V5, mouse monoclonal	Thermo Fisher Scientific	R960. RRID:AB_2556564	1:5000
Antibody	Anti-mouse IgG (H+L) conjugated to AlexaFluor 488, goat polyclonal	Thermo Fisher Scientific	A11001, RRID:AB_2534069	1:500
Antibody	Anti-rabbit IgG (H+L) conjugated to Cy3, goat polyclonal	Thermo Fisher Scientific	A10520, RRID:AB_10563288	1:500
Antibody	Anti-mouse IgG (H+L)-HRP conjugate, goat polyclonal	Bio-Rad	170–6516, RRID:AB_11125547	1:10000
Chemical compound, drug	Hygromycin B	Roth	CP13.4	
Chemical compound, drug	Zeocin	Life Technologies	R25001	
Chemical compound, drug	Doxycycline (DOX)	Clontech	631311	
Chemical compound, drug	Calyculin A (CalA)	LC Laboratories	C-3987	
Chemical compound, drug	Okadaic acid (OA)	Merck	O9381	
Chemical compound, drug	PF670462	Tocris Bio-Techne	3316	
Chemical compound, drug	Cycloheximide (CHX)	PanReac AppliChem	A0879	

Continued on next page

Continued

Reagent type (species) or resource	Designation	Source or reference	Identifiers	Additional information
Chemical compound, drug	Thymidine	Merck	T9250	
Chemical compound, drug	Nocodazole	Merck	SML1665	
Recombinant DNA reagent	pcDNA4/TO	Life Technologies	V1020-20	
Commercial assay or kit	PCR Cleanup Kit	Macherey-Nagel	740609	
Commercial assay or kit	GeneJET Plasmid Extraction Kit	Thermo Fisher Scientific	K0503	
Commercial assay or kit	Xfect Transfection Reagent	Takara Bio	631317	
Commercial assay or kit	ProLong Glass Antifade Mountant with NucBlue	Thermo Fisher Scientific	P36983	
Software, algorithm	Fiji (ImageJ)	NIH	https://imagej.nih.gov/ij/	
Software, algorithm	GraphPad Prism 10	GraphPad Software, Inc, La Jolla, CA, USA	http://www.graphpad.com/	
Software, algorithm	Nikon Imaging	Nikon Europe B.V., Amstelveen, Netherlands	https://www.microscope.healthcare.nikon.com/en_EU/products/software/nis-elements	

Plasmids

Plasmids were constructed as previously described (***Marzoll et al., 2022***). Briefly, restriction digestion, dephosphorylation of vector backbone, and ligation were performed as recommended by New England Biolabs (NEB). Linear DNA was purified using NucleoSpin Gel and PCR Clean-up kit from Macherey-Nagel. Plasmids were extracted with GeneJET Plasmid Miniprep kit from Thermo Fisher Scientific. For cloning with overlapping regions (restriction enzyme-free cloning), enzymes (Q5 DNA polymerase, restriction enzyme DpnI, and T4 DNA polymerase) were obtained from NEB. DpnI digestion and exonuclease reaction with T4 DNA polymerase were performed in NEBuffer 2.1. *Escherichia coli* were transformed with exonuclease-treated PCR product(s) to facilitate in vivo plasmid assembly via overlapping DNA ends. pcDNA4/TO-derived vectors were constructed by cloning the coding regions of the human CK1δ1 splice variant, referred to as CK1δ throughout the manuscript, and CK1ε, downstream of the CMV-TetO2 promoter, which allows for DOX-inducible protein expression in cells harboring the tetracycline-repressor cassette (tx; i.e. U2OStx) and constitutively high expression in cells without the tetracycline-repressor cassette (i.e. HEK293T). Mutations (CK1δ1-K38R) and C-terminal FLAG-tags were introduced via ligation-free overlap cloning. All plasmid DNA sequences were sequence-verified prior to use.

Cell culture and stable cell line generation

T-REx-U2OS (U2OStx; Life Technologies) and HEK293T (ATCC) cells were maintained in Dulbecco's Modified Eagle Medium (DMEM) supplemented with 10% fetal bovine serum (FBS) and 1× Penicillin-Streptomycin (Pen-Strep). Cell culture reagents were obtained from Life Technologies. Cells were grown and maintained at 37°C in a humidified incubator containing 5% CO_2. Cell lines were sourced from their respective suppliers, rapidly expanded, and low-passage stocks were stored in cryopreservation. These low-passage stocks were used as the starting material for downstream experiments and cell line generation. To control for mycoplasma contamination, all cell lines were routinely tested at least twice a year using a PCR-based mycoplasma detection assay.

For plasmid transfection, U2OStx cells were transfected with Xfect Transfection Reagent (Takara Bio Inc, Cat# 6313317) following the manufacturer's protocol, whereas HEK293T cells were transfected with polyethylenimine (made in-house) following the conventional protocol. To generate stable U2OStx cell lines, basal U2OStx cells were seeded in a 24-well plate and grown to confluence overnight. Cells were transfected with pcDNA4/TO vectors containing coding regions of CK1δ, CK1δ-K38R, or CK1ε with C-terminal FLAG epitopes. Stable transfectants were selected by growing cells to sub-confluence in complete media supplemented with 50 µg/mL hygromycin and 100 µg/mL zeocin

(Invitrogen, Cat# R25001) over the course of 2–3 weeks. Resulting single cell colonies after selection were isolated for further experimentation as previously described. To induce protein overexpression, cells were treated with 10 ng/mL DOX.

Immunofluorescence

U2OStx, U2OStx_CK1δ, or U2OStx_mK2-CRY1 cells were seeded on 12 mm #1.0 glass coverslips (VWR, Cat# 631-1577P). IF was done either post-seeding or post-plasmid transfection and 24 hr post-DOX induction. Cells were washed with PBS and fixed with 4% paraformaldehyde for 10 min at room temperature. Cells were permeabilized with PBS+0.1% Triton X-100 for 10 min, then washed three times and blocked with PBS+5% heat-inactivated FBS for 1 hr. Cells were then treated with either mouse monoclonal anti-CK1δ (abcam ab85320, clone AF12G4, 1:5000) or mouse monoclonal anti-FLAG antibody (Sigma-Aldrich F3165, 1:200), or rabbit polyclonal anti-PCNT (abcam ab4448, generous gift from Dr. Cornelia Sala and Prof. Elmar Schiebel, 1:500), or rabbit polyclonal anti-hPER2 (in-house, 1:50) diluted in PBS+3% BSA+0.25% Tween 20 for 1 hr to detect endogenous or overexpressed CK1δ, respectively. This was followed by washing with PBS and treatment with the corresponding secondary antibody goat anti-mouse conjugated to Alexa Fluor488 (AF488; Thermo Fisher Scientific A11001, 1:500) or goat anti-rabbit conjugated to Cy3 (Thermo Fisher Scientific A10520, 1:500) diluted in PBS+3% BSA+0.25% Tween 20 for 1 hr at 37°C. Cells were again washed three times, then mounted onto glass slides with ProLong Glass Antifade Mountant with NucBlue (Thermo Fisher Scientific P36983) and sealed with nail polish.

Fluorescence microscopy

For microscopy of fluorescently tagged proteins and IF, a widefield Nikon Ni-E microscope was used (Nikon Imaging Center, Heidelberg), at a ×60 magnification oil immersion objective. The corresponding filter sets for DAPI, AF488, Cy3, and mK2 were then used to visualize the specific signal from each fluorophore used. Exposure times were optimized and kept constant within each experiment to obtain comparable fluorescence intensities between treatment conditions (i.e. no treatment vs. CHX+PF670462 treatment). For image acquisition, the central focal plane was determined and images were taken at 0.3 µm z-steps to a total of 11 steps.

Digital image analysis

To analyze the resulting micrographs, built-in programs in Fiji were used. To quantify CK1δ localization at the centrosome, the PCNT channel was used to detect the subcellular localization of the centrosome. The signal intensity at the corresponding CK1δ and FLAG channels was then quantified and background-subtracted. These values were then tabulated for statistical analysis via Welch's t-test using the built-in analysis in GraphPad Prism 10. The resulting data was visualized using GraphPad Prism 10.

To perform the line plot analysis, a region of interest was selected using the line selection tool followed by using the built-in plot profile function in Fiji. These data were then visualized using GraphPad Prism 10.

Immunoblotting

Protein extraction was performed using an in-house lysis buffer (25 mM Tris-HCl, pH 8.0, 150 mM NaCl, 0.5% Triton X-100, 2 mM EDTA, 1 mM NaF, freshly added protease inhibitors: 1 mM phenylmethylsulfonyl fluoride, leupeptin [5 µg/mL], and pepstatin A [5 µg/mL]) according to the conventional protocol. Briefly, cells were scraped and the sample was collected via centrifugation. The sample was incubated in ice-cold lysis buffer on ice for 10 min and then incubated in a sonicated water bath for 10 min. Samples were centrifuged at 16,000×*g*, 4°C, for 15 min taking the supernatant. Protein concentration was quantified via NanoDrop (NP80, Implen). For immunoblot analysis, protein samples were analyzed using SDS-polyacrylamide gel electrophoresis and transferred to a nitrocellulose membrane (cytiva, Amersham Protran, 0.45 µm pore size) via semi-dry blotting. To control for protein loading, membranes were stained with Ponceau S. Membranes were typically incubated in primary antibody at 4°C overnight and in secondary antibody conjugated to horseradish peroxidase at room temperature for 2 hr. The following primary antibodies were used: anti-FLAG (Sigma-Aldrich F3165, 1:5000, mouse monoclonal), anti-CK1δ (abcam AF12G4, 1:5000, mouse monoclonal), and the

following secondary antibody was used for luminescent detection: goat anti-mouse IgG (H+L)-HRP conjugate (Bio-Rad 170-6516, 1:10000). For decoration, membranes were incubated in decoration buffer (100 mM Tris-HCl pH 8.5, 2.2×10^{-2}% [wt/vol] luminol, 3.3×10^{-3}% [wt/vol] coumaric acid, 9.0×10^{-3}% [vol/vol] H_2O_2) and exposed for a time series to X-ray films (Fujifilm). Films were then developed using a medical film processor (Konica Minolta). Densitometric analysis of immunoblots was done using the built-in module in Fiji. The results were measured and plotted onto GraphPad Prism for downstream analysis (i.e. plotting densitometric signal over time post-CHX chase).

Phosphatase inhibition and CHX chase

To characterize phosphatase activity, cells were treated with either CalA or OA. To inhibit phosphatases over a time course, cells were treated with 80 nM CalA (LC Labs Cat# C-3987) for 60, 20, 6, and 0 (untreated) min. All chemical treatments were performed with the corresponding solvent (vehicle) control such as DMSO for CalA and H_2O for CHX and PF670462.

Unless otherwise stated, induction of protein expression was typically performed by the addition of 10 ng/mL DOX (Thermo Fisher Scientific, Cat# 631311) 24 hr prior to downstream experiments. To arrest protein translation for a CHX chase, CHX was added to our cells to a final concentration of 10 µg/mL. Untreated samples were taken as the 0 min CHX sample. Samples were then taken at 15, 30, 45, 60, and 90 min post-CHX for protein extraction and immunoblotting. To inhibit CK1δ or CK1ε, cells were treated with 1 µM PF670462 (Tocris Biosciences Cat# 3316) for 4 hr prior to immunoblotting and IF.

Cell-cycle arrest protocol

Cell-cycle arrest protocol was adapted from ***Apraiz et al., 2017***. For both the S phase release and cell-cycle arrest, U2OStx or U2OStx_CK1δ cells were seeded onto four 10 cm dishes to reach 50% confluence. To release cells from S phase, a double thymidine (THY, final concentration of 2 mM) was used as follows (see ***Figure 5A***): 24 hr post-seeding, cells were treated with THY for 18 hr, released into normal media for 6 hr, treated with THY for a second block for 12 hr. Cells were then released from the second THY block and sampled at 0, 1, and 2 hr post-release.

To arrest cells in either G1/S or G2/M, either a double THY or a THY-nocodazole block, respectively, was used. For the unsynchronized sample, no additional treatment was performed (see ***Figure 5C***). For both the G1- and G2-arrested samples, after 24 hr post-seeding, cells were treated with THY (final concentration of 2 mM) for 18 hr followed by a release into normal media for 6 hr. To arrest cells in G1, cells were treated with a second THY block for 12 hr. To arrest cells in G2, cells were treated with nocodazole (NOC, final concentration of 50 ng/mL) for 12 hr. For the G2/M-arrested cells, an additional mitotic shake-off was performed to enrich the sample for cells in mid-mitosis that are loosely attached to the culture surface (***Schorl and Sedivy, 2007***). To induce CK1δ, DOX induction was performed on all samples 24 hr prior to the end of either the double THY or THY-NOC treatments.

Materials availability

Plasmids and cell lines generated in this study are available from the lead contact, Michael Brunner (michael.brunner@bzh.uni-heidelberg.de) with a completed materials transfer agreement.

Acknowledgements

We thank Alessia Ruggieri and Michael Knop for providing mKate2 and mNeonGreen templates, respectively. We also thank Cornelia Sala and Elmar Schiebel for the anti-PCNT antibody. This work was supported by the Deutsche Forschungsgemeinschaft, TRR186.

Additional information

Funding

Funder	Grant reference number	Author
Deutsche Forschungsgemeinschaft	TRR 186	Michael Brunner

The funders had no role in study design, data collection and interpretation, or the decision to submit the work for publication.

Author contributions

Fidel Emmanuel Serrano, Conceptualization, Resources, Data curation, Formal analysis, Supervision, Validation, Investigation, Visualization, Methodology, Writing – original draft, Project administration, Writing – review and editing; Bianca Ruppert, Resources, Methodology; Axel CR Diernfellner, Data curation, Supervision, Investigation, Methodology, Project administration, Writing – review and editing; Michael Brunner, Conceptualization, Supervision, Funding acquisition, Writing – original draft, Project administration, Writing – review and editing

Author ORCIDs

Fidel Emmanuel Serrano https://orcid.org/0000-0001-8906-9343
Axel CR Diernfellner https://orcid.org/0000-0001-6560-2318
Michael Brunner https://orcid.org/0000-0001-9798-3047

Peer review material

Version of Record:
Reviewer #1 (Public review): https://doi.org/10.7554/eLife.112381.3.sa1
Reviewer #2 (Public review): https://doi.org/10.7554/eLife.112381.3.sa2
Author response https://doi.org/10.7554/eLife.112381.3.sa3

Reviewed preprint v2
Reviewer #1 (Public review): https://doi.org/10.7554/eLife.112381.2.sa2
Reviewer #2 (Public review): https://doi.org/10.7554/eLife.112381.2.sa1
Author response: https://doi.org/10.7554/eLife.112381.2.sa0
eLife Assessment https://doi.org/10.7554/eLife.112381.2.sa3

Reviewed preprint v1
Reviewer #1 (Public review): https://doi.org/10.7554/eLife.112381.1.sa2
Reviewer #2 (Public review): https://doi.org/10.7554/eLife.112381.1.sa1
Author response: https://doi.org/10.7554/eLife.112381.1.sa0
eLife Assessment https://doi.org/10.7554/eLife.112381.1.sa3

Additional files

Supplementary files

MDAR checklist

Data availability

The data supporting the findings of this study are available within the article. This study includes no data deposited in external repositories.

References

Apraiz A, Mitxelena J, Zubiaga A. 2017. Studying cell cycle-regulated gene expression by two complementary cell synchronization protocols. *Journal of Visualized Experiments* **6**:55745. DOI: https://doi.org/10.3791/55745, PMID: 28654080

Aquino Perez C, Burocziova M, Jenikova G, Macurek L. 2021. CK1-mediated phosphorylation of FAM110A promotes its interaction with mitotic spindle and controls chromosomal alignment. *EMBO Reports* **22**:e51847. DOI: https://doi.org/10.15252/embr.202051847, PMID: 34080749

Arseni C, Samiotaki M, Panayotou G, Simos G, Mylonis I. 2024. Combinatorial regulation by ERK1/2 and CK1δ protein kinases leads to HIF-1α association with microtubules and facilitates its symmetrical distribution during mitosis. *Cellular and Molecular Life Sciences* **81**:72. DOI: https://doi.org/10.1007/s00018-024-05120-7, PMID: 38300329

Badura L, Swanson T, Adamowicz W, Adams J, Cianfrogna J, Fisher K, Holland J, Kleiman R, Nelson F, Reynolds L, St Germain K, Schaeffer E, Tate B, Sprouse J. 2007. An inhibitor of casein kinase I epsilon induces phase delays in circadian rhythms under free-running and entrained conditions. *The Journal of Pharmacology and Experimental Therapeutics* **322**:730–738. DOI: https://doi.org/10.1124/jpet.107.122846, PMID: 17502429

Behrend L, Stöter M, Kurth M, Rutter G, Heukeshoven J, Deppert W, Knippschild U. 2000. Interaction of casein kinase 1 delta (CK1delta) with post-Golgi structures, microtubules and the spindle apparatus. *European Journal of Cell Biology* **79**:240–251. DOI: https://doi.org/10.1078/s0171-9335(04)70027-8, PMID: 10826492

Cao X, Yang Y, Selby CP, Liu Z, Sancar A. 2021. Molecular mechanism of the repressive phase of the mammalian circadian clock. *PNAS* **118**:e2021174118. DOI: https://doi.org/10.1073/pnas.2021174118, PMID: 33443219

Cegielska A, Gietzen KF, Rivers A, Virshup DM. 1998. Autoinhibition of casein kinase I epsilon (CKI epsilon) is relieved by protein phosphatases and limited proteolysis. *The Journal of Biological Chemistry* **273**:1357–1364. DOI: https://doi.org/10.1074/jbc.273.3.1357, PMID: 9430669

Cruciat CM. 2014. Casein kinase 1 and Wnt/β-catenin signaling. *Current Opinion in Cell Biology* **31**:46–55. DOI: https://doi.org/10.1016/j.ceb.2014.08.003, PMID: 25200911

Cullati SN, Akizuki K, Chen J-S, Johnson JL, Yaron-Barir TM, Cantley LC, Gould KL. 2024. Substrate displacement of CK1 C-termini regulates kinase specificity. *Science Advances* **10**:eadj5185. DOI: https://doi.org/10.1126/sciadv.adj5185, PMID: 38728403

DeMaggio AJ, Lindberg RA, Hunter T, Hoekstra MF. 1992. The budding yeast HRR25 gene product is a casein kinase I isoform. *PNAS* **89**:7008–7012. DOI: https://doi.org/10.1073/pnas.89.15.7008, PMID: 1495994

Etchegaray J-P, Machida KK, Noton E, Constance CM, Dallmann R, Di Napoli MN, DeBruyne JP, Lambert CM, Yu EA, Reppert SM, Weaver DR. 2009. Casein kinase 1 delta regulates the pace of the mammalian circadian clock. *Molecular and Cellular Biology* **29**:3853–3866. DOI: https://doi.org/10.1128/MCB.00338-09, PMID: 19414593

Flotow H, Graves PR, Wang AQ, Fiol CJ, Roeske RW, Roach PJ. 1990. Phosphate groups as substrate determinants for casein kinase I action. *The Journal of Biological Chemistry* **265**:14264–14269 PMID: 2117608.

Gao ZH, Seeling JM, Hill V, Yochum A, Virshup DM. 2002. Casein kinase I phosphorylates and destabilizes the beta-catenin degradation complex. *PNAS* **99**:1182–1187. DOI: https://doi.org/10.1073/pnas.032468199, PMID: 11818547

Görl M, Merrow M, Huttner B, Johnson J, Roenneberg T, Brunner M. 2001. A PEST-like element in FREQUENCY determines the length of the circadian period in *Neurospora crassa*. *The EMBO Journal* **20**:7074–7084. DOI: https://doi.org/10.1093/emboj/20.24.7074, PMID: 11742984

Graves PR, Roach PJ. 1995. Role of COOH-terminal phosphorylation in the regulation of casein kinase I delta. *The Journal of Biological Chemistry* **270**:21689–21694. DOI: https://doi.org/10.1074/jbc.270.37.21689, PMID: 7665585

Greer YE, Rubin JS. 2011. Casein kinase 1 delta functions at the centrosome to mediate Wnt-3a-dependent neurite outgrowth. *The Journal of Cell Biology* **192**:993–1004. DOI: https://doi.org/10.1083/jcb.201011111, PMID: 21422228

Greer YE, Westlake CJ, Gao B, Bharti K, Shiba Y, Xavier CP, Pazour GJ, Yang Y, Rubin JS. 2014. Casein kinase 1δ functions at the centrosome and Golgi to promote ciliogenesis. *Molecular Biology of the Cell* **25**:1629–1640. DOI: https://doi.org/10.1091/mbc.E13-10-0598, PMID: 24648492

Greer YE, Gao B, Yang Y, Nussenzweig A, Rubin JS. 2017. Lack of casein kinase 1 delta promotes genomic instability - the accumulation of DNA damage and down-regulation of checkpoint kinase 1. *PLOS ONE* **12**:e0170903. DOI: https://doi.org/10.1371/journal.pone.0170903, PMID: 28125685

Gross SD, Anderson RA. 1998. Casein kinase I: spatial organization and positioning of a multifunctional protein kinase family. *Cellular Signalling* **10**:699–711. DOI: https://doi.org/10.1016/s0898-6568(98)00042-4, PMID: 9884021

Grozav AG, Chikamori K, Kozuki T, Grabowski DR, Bukowski RM, Willard B, Kinter M, Andersen AH, Ganapathi R, Ganapathi MK. 2009. Casein kinase I delta/epsilon phosphorylates topoisomerase IIalpha at serine-1106 and modulates DNA cleavage activity. *Nucleic Acids Research* **37**:382–392. DOI: https://doi.org/10.1093/nar/gkn934, PMID: 19043076

Harold RL, Tulsian NK, Narasimamurthy R, Yaitanes N, Ayala Hernandez MG, Lee HW, Crosby P, Tripathi SM, Virshup DM, Partch CL. 2024. Isoform-specific C-terminal phosphorylation drives autoinhibition of casein kinase 1. *PNAS* **121**:e2415567121. DOI: https://doi.org/10.1073/pnas.2415567121, PMID: 39356670

Inuzuka H, Tseng A, Gao D, Zhai B, Zhang Q, Shaik S, Wan L, Ang XL, Mock C, Yin H, Stommel JM, Gygi S, Lahav G, Asara J, Xiao Z-XJ, Kaelin WG Jr, Harper JW, Wei W. 2010. Phosphorylation by casein kinase I promotes the turnover of the Mdm2 oncoprotein via the SCF(beta-TRCP) ubiquitin ligase. *Cancer Cell* **18**:147–159. DOI: https://doi.org/10.1016/j.ccr.2010.06.015, PMID: 20708156

Ishihara H, Martin BL, Brautigan DL, Karaki H, Ozaki H, Kato Y, Fusetani N, Watabe S, Hashimoto K, Uemura D, Hartshorne DJ. 1989. Calyculin A and okadaic acid: inhibitors of protein phosphatase activity. *Biochemical and Biophysical Research Communications* **159**:871–877. DOI: https://doi.org/10.1016/0006-291x(89)92189-x, PMID: 2539153

Jiang K, Liu Y, Fan J, Epperly G, Gao T, Jiang J, Jia J. 2014. Hedgehog-regulated atypical PKC promotes phosphorylation and activation of Smoothened and Cubitus interruptus in *Drosophila*. *PNAS* **111**:E4842–E4850. DOI: https://doi.org/10.1073/pnas.1417147111, PMID: 25349414

Johnson LN, Noble MEM, Owen DJ. 1996. Active and inactive protein kinases: structural basis for regulation. *Cell* **85**:149–158. DOI: https://doi.org/10.1016/s0092-8674(00)81092-2, PMID: 8612268

Johnson AE, Chen JS, Gould KL. 2013. CK1 is required for a mitotic checkpoint that delays cytokinesis. *Current Biology* **23**:1920–1926. DOI: https://doi.org/10.1016/j.cub.2013.07.077, PMID: 24055157

Kim HS, Fernandes G, Lee CW. 2016. Protein phosphatases involved in regulating mitosis: facts and hypotheses. *Molecules and Cells* **39**:654–662. DOI: https://doi.org/10.14348/molcells.2016.0214, PMID: 27669825

Klimczak LJ, Farini D, Lin C, Ponti D, Cashmore AR, Giuliano G. 1995. Multiple isoforms of Arabidopsis casein kinase I combine conserved catalytic domains with variable carboxyl-terminal extensions. *Plant Physiology* **109**:687–696. DOI: https://doi.org/10.1104/pp.109.2.687, PMID: 7480353

Lee C, Etchegaray JP, Cagampang FRA, Loudon ASI, Reppert SM. 2001. Posttranslational mechanisms regulate the mammalian circadian clock. *Cell* **107**:855–867. DOI: https://doi.org/10.1016/S0092-8674(01)00610-9, PMID: 11779462

Lee H, Chen R, Kim H, Etchegaray J-P, Weaver DR, Lee C. 2011. The period of the circadian oscillator is primarily determined by the balance between casein kinase 1 and protein phosphatase 1. *PNAS* **108**:16451–16456. DOI: https://doi.org/10.1073/pnas.1107178108, PMID: 21930935

Liu F, Virshup DM, Nairn AC, Greengard P. 2002. Mechanism of regulation of casein kinase I activity by group I metabotropic glutamate receptors. *The Journal of Biological Chemistry* **277**:45393–45399. DOI: https://doi.org/10.1074/jbc.M204499200, PMID: 12223474

Machida YJ, Dutta A. 2007. The APC/C inhibitor, Emi1, is essential for prevention of rereplication. *Genes & Development* **21**:184–194. DOI: https://doi.org/10.1101/gad.1495007, PMID: 17234884

Marzoll D, Serrano FE, Shostak A, Schunke C, Diernfellner ACR, Brunner M. 2022. Casein kinase 1 and disordered clock proteins form functionally equivalent, phospho-based circadian modules in fungi and mammals. *PNAS* **119**:e2118286119. DOI: https://doi.org/10.1073/pnas.2118286119, PMID: 35217617

Matthews HK, Bertoli C, de Bruin RAM. 2022. Cell cycle control in cancer. *Nature Reviews. Molecular Cell Biology* **23**:74–88. DOI: https://doi.org/10.1038/s41580-021-00404-3, PMID: 34508254

Milne DM, Looby P, Meek DW. 2001. Catalytic activity of protein kinase CK1 delta (casein kinase 1delta) is essential for its normal subcellular localization. *Experimental Cell Research* **263**:43–54. DOI: https://doi.org/10.1006/excr.2000.5100, PMID: 11161704

Narasimamurthy R, Hunt SR, Lu Y, Fustin J-M, Okamura H, Partch CL, Forger DB, Kim JK, Virshup DM. 2018. CK1δ/ε protein kinase primes the PER2 circadian phosphoswitch. *PNAS* **115**:5986–5991. DOI: https://doi.org/10.1073/pnas.1721076115, PMID: 29784789

Nasa I, Kettenbach AN. 2018. Coordination of protein kinase and phosphoprotein phosphatase activities in mitosis. *Frontiers in Cell and Developmental Biology* **6**:30. DOI: https://doi.org/10.3389/fcell.2018.00030, PMID: 29623276

Nilsson J. 2019. Protein phosphatases in the regulation of mitosis. *The Journal of Cell Biology* **218**:395–409. DOI: https://doi.org/10.1083/jcb.201809138, PMID: 30446607

Penas C, Ramachandran V, Simanski S, Lee C, Madoux F, Rahaim RJ, Chauhan R, Barnaby O, Schurer S, Hodder P, Steen J, Roush WR, Ayad NG. 2014. Casein kinase 1δ-dependent Wee1 protein degradation. *The Journal of Biological Chemistry* **289**:18893–18903. DOI: https://doi.org/10.1074/jbc.M114.547661, PMID: 24817118

Penas C, Govek E-E, Fang Y, Ramachandran V, Daniel M, Wang W, Maloof ME, Rahaim RJ, Bibian M, Kawauchi D, Finkelstein D, Han J-L, Long J, Li B, Robbins DJ, Malumbres M, Roussel MF, Roush WR, Hatten ME, Ayad NG. 2015. Casein kinase 1δ is an APC/C(Cdh1) substrate that regulates cerebellar granule cell neurogenesis. *Cell Reports* **11**:249–260. DOI: https://doi.org/10.1016/j.celrep.2015.03.016, PMID: 25843713

Peters JM. 2002. The anaphase-promoting complex. *Molecular Cell* **9**:931–943. DOI: https://doi.org/10.1016/S1097-2765(02)00540-3

Peters JM. 2006. The anaphase promoting complex/cyclosome: a machine designed to destroy. *Nature Reviews. Molecular Cell Biology* **7**:644–656. DOI: https://doi.org/10.1038/nrm1988, PMID: 16896351

Rivers A, Gietzen KF, Vielhaber E, Virshup DM. 1998. Regulation of casein kinase I epsilon and casein kinase I delta by an in vivo futile phosphorylation cycle. *The Journal of Biological Chemistry* **273**:15980–15984. DOI: https://doi.org/10.1074/jbc.273.26.15980, PMID: 9632646

Roth A, Gihring A, Bischof J, Pan L, Oswald F, Knippschild U. 2022. CK1 is a druggable regulator of microtubule dynamics and microtubule-associated processes. *Cancers* **14**:1345. DOI: https://doi.org/10.3390/cancers14051345, PMID: 35267653

Schittek B, Sinnberg T. 2014. Biological functions of casein kinase 1 isoforms and putative roles in tumorigenesis. *Molecular Cancer* **13**:231. DOI: https://doi.org/10.1186/1476-4598-13-231, PMID: 25306547

Schorl C, Sedivy JM. 2007. Analysis of cell cycle phases and progression in cultured mammalian cells. *Methods* **41**:143–150. DOI: https://doi.org/10.1016/j.ymeth.2006.07.022, PMID: 17189856

Serrano FE, Marzoll D, Ruppert B, Diernfellner AC, Brunner M. 2026. Nuclear CK1δ as a critical determinant of PER:CRY complex dynamics and circadian period. *eLife* **15**:e110786. DOI: https://doi.org/10.7554/eLife.110786.2

Sillibourne JE, Milne DM, Takahashi M, Ono Y, Meek DW. 2002. Centrosomal anchoring of the protein kinase CK1delta mediated by attachment to the large, coiled-coil scaffolding protein CG-NAP/AKAP450. *Journal of Molecular Biology* **322**:785–797. DOI: https://doi.org/10.1016/s0022-2836(02)00857-4, PMID: 12270714

Sivakumar S, Gorbsky GJ. 2015. Spatiotemporal regulation of the anaphase-promoting complex in mitosis. *Nature Reviews. Molecular Cell Biology* **16**:82–94. DOI: https://doi.org/10.1038/nrm3934, PMID: 25604195

Swingle M, Ni L, Honkanen RE. 2006. Small-molecule inhibitors of ser/thr protein phosphatases: specificity, use and common forms of abuse. In: Swingle M (Ed). *Protein Phosphatase Protocols*. New Jersey: Humana Press. p. 23–38. DOI: https://doi.org/10.1385/1-59745-267-X:23

Takahashi JS. 2017. Transcriptional architecture of the mammalian circadian clock. *Nature Reviews. Genetics* **18**:164–179. DOI: https://doi.org/10.1038/nrg.2016.150, PMID: 27990019

Winter M, Milne D, Dias S, Kulikov R, Knippschild U, Blattner C, Meek D. 2004. Protein kinase CK1delta phosphorylates key sites in the acidic domain of murine double-minute clone 2 protein (MDM2) that regulate p53 turnover. *Biochemistry* **43**:16356–16364. DOI: https://doi.org/10.1021/bi0489255, PMID: 15610030

Xu P, Ianes C, Gärtner F, Liu C, Burster T, Bakulev V, Rachidi N, Knippschild U, Bischof J. 2019. Structure, regulation, and (patho-)physiological functions of the stress-induced protein kinase CK1 delta (CSNK1D). *Gene* **715**:144005. DOI: https://doi.org/10.1016/j.gene.2019.144005, PMID: 31376410

Zhao B, Li L, Tumaneng K, Wang CY, Guan KL. 2010. A coordinated phosphorylation by Lats and CK1 regulates YAP stability through SCF(beta-TRCP). *Genes & Development* **24**:72–85. DOI: https://doi.org/10.1101/gad.1843810, PMID: 20048001